Defective proventriculus specifies the ocellar region in the *Drosophila* head

Takeshi Yorimitsu, Naruto Kiritooshi, Hideki Nakagoshi

Graduate School of Natural Science and Technology, Okayama University, 3-1-1 Tsushima-naka, Kita-ku, Okayama 700-8530, Japan

Correspondence: Hideki Nakagoshi

Graduate School of Natural Science and Technology, Okayama University, 3-1-1

Tsushima-naka, Kita-ku, Okayama 700-8530, Japan

TEL: (+81)-86-251-7875　FAX: (+81)-86-251-7876

E-mail: goshi@cc.okayama-u.ac.jp

Abstract

A pair of the *Drosophila* eye-antennal disc gives rise to four distinct organs (eyes, antennae, maxillary palps, and ocelli) and surrounding head cuticle. Developmental processes of this imaginal disc provide an excellent model system to study the mechanism of regional specification and subsequent organogenesis. The dorsal head capsule (vertex) of adult *Drosophila* is divided into three morphologically distinct subdomains: ocellar, frons, and orbital. The homeobox gene *orthodenticle* (*otd*) is required for head vertex development, and mutations that reduce or abolish *otd* expression in the vertex primordium lead to ocelliless flies. The homeodomain-containing transcriptional repressor Engrailed (En) is also involved in ocellar specification, and the En expression is completely lost in *otd* mutants. However, the molecular mechanism of ocellar specification remains elusive. Here, we provide evidence that the homeobox gene *defective proventriculus* (*dve*) is a downstream effector of Otd, and also that the repressor activity of Dve is required for *en* activation through a relief-of-repression mechanism. Furthermore, the Dve activity is involved in repression of the frons identity in an incoherent feedforward loop of Otd and Dve.

Key words: *Drosophila*; eye; orthodenticle; hedgehog; engrailed; Iroquois

Introduction

In the process of pattern formation, a developmental field is subdivided into discrete domains, and spatial and temporal pattern of precisely regulated gene expression is crucial for proper organ development. *Drosophila* eye-antennal discs represent an excellent model system for studying pattern formation and regional specification in a multicellular field because this single primordium gives rise to four distinct organs (eyes, antennae, maxillary palps, and ocelli) and surrounding head cuticle (Kenyon et al., 2003).

It has been shown that pattern formation is differentially regulated in the head and trunck regions of the early embryo (reviewed in (Cohen and Jurgens, 1991; Finkelstein and Perrimon, 1991). The adult head is also specified differentially from the thoracic appendage. The thoracic discs originate from a single embryonic segment, whereas the head capsule is derived from specific primordia within the eye-antennal disc, which is formed from multiple embryonic head segments (Hartenstein and Jan, 1992; Jurgens and Hartenstein, 1993).

The dorsal head capsule (vertex) of adult *Drosophila* is occupied by a characteristic set of structural features that lie between the compound eyes, which is divided into three morphologically distinct subdomains: ocellar, frons, and orbital. The ocelli (simple light-sensitive organs) are located in the medial subdomain (triangular ocellar cuticle). The mediolateral subdomain (frons cuticle) lies immediately adjacent to the ocellar region, and consists of a series of closely spaced parallel ridges. The lateral subdomain (orbital cuticle) occupies the space between the frons and the compound eyes, which has a stereotypical array of macrochaetes (Haynie and Bryant, 1986).

Pattern formation in the head vertex requires the homeodomain protein Orthodenticle (Otd). During the second larval instar, Otd is ubiquitously expressed in the eye-antennal discs and it is gradually restricted in the vertex primordium until early third larval instar (Royet and Finkelstein, 1995; Royet and Finkelstein, 1997). The restricted expression of *otd* initially depends on Wingless (Wg) and Hedgehog (Hh) signaling, then these signals become redundant and a positive autoregulatory loop, by Otd itself, sets in to maintain *otd* expression during subsequent stages of vertex primordium development (Blanco et al., 2009; Royet and Finkelstein, 1996). In late

third larval instar, retinal determination genes, *sine oculis* (*so*) and *eyes absent* (*eya*), and a transcriptional repressor, *engrailed* (*en*), are induced in the medial subdomain to form ocelli (Blanco et al., 2009; Punzo et al., 2002; Royet and Finkelstein, 1995; Royet and Finkelstein, 1996).

The homeobox gene *defective proventriculus* (*dve*) is expressed in various tissues including the head primordium and involved in transcriptional repression. For instance, *dve* expression itself is negatively autoregulated in the larval midgut (Nakagoshi et al., 1998). Expression of Notch target genes, *wg*, *cut (ct)*, and *dAP-2*, are repressed by Dve at the dorso-ventral and segment boundaries of wing and leg discs, respectively (Kölzer et al., 2003; Nakagoshi et al., 2002; Shirai et al., 2007). In photoreceptor (PR) cells, Dve is expressed in outer PR (R1-R6) and yellow-type inner PR (yR7). Rhodopsin 3 (Rh3) is expressed in pale-type R7 (pR7) by the Otd activity and it is repressed in yR7 by the Dve activity (Johnston et al., 2011; Tahayato et al., 2003). In this study, we have examined *dve* functions for ocelli formation. We present evidence that the *dve* gene is a downstream target of Otd in the vertex primordium, and also that the repressor activity of Dve is crucial for maintenance of *hh* expression to specify the ocellar region through a relief-of-repression mechanism. The Dve activity is also required for repression of the frons identity in an incoherent type-1 feedforward loop of Otd and Dve.

Materials and Methods

Fly stocks

Flies were reared on standard yeast/glucose medium at 25^{O}C. Oregon-R flies were used as wild-type controls. The following mutant or marker strains were used: oc^{ya1} (Drosophila Genetic Resource Center, Kyoto), oc^{1}, oc^{2} *FRT19A*, otd^{YH13}*FRT19A*, *hh-lacZ* (Bloomington Stock Center), *wg-lacZ* (Kassis et al., 1992), iro^{DFM3}, $mirr^{cre2}$ *(mirr-lacZ)*, ara^{rF209} *(ara-lacZ)* (Gómez-Skarmeta et al., 1996), dve^{1} (dve^{1}*-lacZ)*, dve^{E38}, *FRT42D* dve^{E38} (Nakagoshi et al., 1998; Nakagoshi et al., 2002), *FRT42D* dve^{L186} (Terriente et al., 2008), and dve^{E181} (Nakagawa et al., 2011).

The following GAL4/UAS strains were used: *tubP-GAL4*, $tubP\text{-}GAL80^{ts}$, *ptc-GAL4*,

UAS-GFP.S65T, UAS-otd (Bloomington Stock Center), *Ay-GAL4.25 UAS-GFP.S65T* (Ito et al., 1997), *dve*^{NP1550}*-GAL4, NP4065* (Hayashi et al., 2002)(DGRC, Kyoto), *UAS-Ci*^{75} (Aza-Blanc et al., 1997), *UAS-HA-Ci*^{155} (Chen et al., 1998), *UAS-ara* (Gómez-Skarmeta et al., 1996), and *UAS-dve-B* (Nakagawa et al., 2011). To knock down the *dve* expression, *UAS-dve-IR* (v109538, Vienna Drosophila RNAi Center) was used.

Mosaic analyses

Mosaic clones were induced with the use of FRT- and FLP-mediated recombination systems (Newsome et al., 2000; Xu and Rubin, 1993). *dve*^{L186} is a small deletion allele that completely removes the gene (Terriente et al., 2008). To generate *dve* null mutant mosaic clones, *y w; FRT42D dve*^{L186}*/ CyO[y*$^{+}$*]* flies were crossed with *y w hs-flp; ey-flp5 FRT42D ubi-GFP[w*$^{+}$*] M(2)53*^{1} or *y w ey-flp2; FRT42D ubi-GFP[w*$^{+}$*]* flies. Homozygous clones for the hypomorphic allele *dve*^{E38} have undetectable Dve proteins in the eye-antennal disc. Mutant clones were generated as a following genotype: *y w hs-flp/ Y; wg-lacZ FRT42D dve*^{E38}*/ ey-FLP5 FRT42D ubi-GFP[w*$^{+}$*] M(2)53*^{1}.

Mutant clones for *oc*^{2} or *otd*^{YH13} were induced with the MARCM system (Lee and Luo, 1999) and positively labeled with membrane tethered CD8::GFP as following genotypes: *y sn*^{3} *oc*^{2} *FRT19A/tub-GAL80 hs-FLP FRT19A; ey-flp5/UAS-mCD8::GFP; tub-GAL4/+* and *w otd*^{YH13} *FRT19A/tub-GAL80 hs-FLP FRT19A; ey-flp5/UAS-mCD8::GFP; tub-GAL4/+*.

Mosaic clones expressing Otd, Ci^{75}, Ci^{155}, Ara, or Dve-B were induced with the Ay-GAL4 system (Ito et al., 1997). *Ay-Gal4.25 UAS-GFP.S65T* flies were crossed with *y w hs-flp; UAS-otd*, *y w hs-flp; UAS-Ci*^{75}, *y w hs-flp; UAS-HA-Ci*^{155}, *y w hs-flp; UAS-ara*, or *y w hs-flp; UAS-dveB* flies, and subjecting the offspring to heat shock at 38°C for 20 min at the first larval instar.

Immunohistochemistry

Larvae were dissected in phosphate-buffered saline (PBS), fixed with 4% formaldehyde/PBS-0.2% Tween20 for 20 min, and washed several times with PBS-0.3% Triton X-100. The following primary antibodies were used: mouse anti-En

4D9 [Developmental Studies Hybridoma Bank (DSHB), 1:200 dilution], mouse anti-Wg 4D4 (DSHB, 1:200), mouse anti-Eya (DSHB, 1:200), mouse anti-β-galactosidase (Promega; 1:200), guinea pig anti-Eyg (1:200) (Aldaz et al., 2003), rabbit anti-Otd (1:500) (Wang et al., 2010), and rabbit anti-Dve (1:5000) (Nakagoshi et al., 1998). FITC-, Cy3- or Cy5-conjugated secondary antibodies (Jackson Immunoresearch) were used for detection. Confocal images were obtained with an OLYMPUS FV300.

Preparation of adult cuticles

Adult flies were briefly washed with 70% ethanol. After removal of the proboscis, soft parts of adult heads were digested with 10% KOH/ PBS, washed with 70% ethanol, and mounted in Permount (Fisher Scientific) (Aldaz et al., 2003). Nomarski images were obtained with a Zeiss AxioVision 3.0, and the photo images were processed using a Photoshop software (Adobe).

Rescue experiments by forced dve-B expression

y NP4065 ct w oc^{1}*/Y; UAS-dve-B/+; tub-GAL80*^{ts}*/+* flies were reared at 18°C by the mid-late third larval instar and then shifted to the restrictive temperature (30°C) for 5 hours to allow GAL4 activity. They were then reared again at 18°C.

Results

dve mutant phenotypes in the ocellar region

A head vertex positions between compound eyes in the most dorsal region. The vertex cuticle can be subdivided into three morphologically distinct domains: ocellar, frons, and orbital. The ocellar region is the most medial triangular cuticle, which contains three ocelli, two large ocellar bristles, and six to eight small interocellar bristles. Adjacent to the ocellar region, frons shows ridged cuticle and has no bristle. The orbital region is the most lateral cuticle, which is flanking to the compound eye and has some macrochaetes (Fig.1 A). The homeobox gene *dve* is expressed in various tissues

including the head primordium (Nakagoshi et al., 1998; Nakagoshi et al., 2002; Shirai et al., 2003; Shirai et al., 2007). In *dve* null mutant heads, the ocellar cuticle was transformed into the frons cuticle and ocelli were completely lost (Fig. 1B).

The homeodomain protein Otd is required for head vertex development, and *otd* mutant heads also show ocelliless phenotype. The previously identified *ocelliless* (*oc*) mutations are allelic to the *otd* locus (Finkelstein et al., 1990; Royet and Finkelstein, 1995). The *oc* mutations are associated with lesions 3' to the *otd* gene and flies hemizygous for a strong *oc* allele ($oc^{\gamma a1}$) cause the loss of both ocellar and frons structures. Flies hemizygous for a weaker *oc* allele (oc^{1}) show a similar phenotype, but more frons cuticle remains (Royet and Finkelstein, 1995) (Figs. 1C, D). Mutant phenotypes for hemizygous $oc^{\gamma a1}$ were clearly different from those of *dve* mutants (Figs. 1B, C). The ridged cuticle of frons and bristles in the ocellar region were not observed in $oc^{\gamma a1}$ mutants, suggesting that the ocelliless phenotype in loss of *otd* function is due to the mis-specification of both frons and ocellar regions.

Otd is sufficient for dve induction but not for en

To examine the relationship between *otd* and *dve*, we compared the expression pattern using the GAL4 enhancer-trap line NP1550, which has a P element insertion upstream of the type-B (*dve-B*) transcription start site of the *dve* gene (Supplementary data, Fig. S1A). NP1550-driven GFP expression (*NP1550>GFP*) was nearly identical to the expression pattern of endogenous Dve protein in the vertex region (Fig. 2A). Otd is also expressed in the entire head vertex region as a similar pattern to that of Dve (Fig. 2B). In oc^{1} mutant discs, Otd expression is particularly reduced in the medial region, which normally gives rise to ocelli, and Dve expression was also reduced (Figs. 2C, D). Expression of an Otd-target gene, *en*, is completely lost in *oc* mutant discs (Royet and Finkelstein, 1995; Figs. 1E, 2D', E'). In $oc^{\gamma a1}$ mutant discs, we could detect residual Dve expression in the head vertex primordium (Fig. 2E).

The greatly reduced Dve expression in $oc^{\gamma a1}$ mutant discs strongly suggests that Otd is an upstream activator of the *dve* gene. To confirm this, we generated *otd* null mutant clones in eye-antennal discs using the MARCM system (Lee and Luo, 1999). In otd^{YH13} or oc^{2} null mutant clones, Dve expression was completely lost in a cell-autonomous manner (Fig. 2F and Figs. S2C, D).

Then, we checked the effect of forced *otd* expression using the Ay-GAL4 system (Ito et al., 1997). In Otd-expressing clones (*Ay>otd*), ectopic Dve expression could also be induced in a cell-autonomous manner, whereas En expression was not induced (Fig. 2G). These results indicate that Otd is necessary and sufficient for Dve expression and also that Otd is indirectly required for En expression.

Two transcripts, *dve-A* and *dve-B*, are transcribed from the *dve* locus, and the *lacZ* reporter expression of the enhancer-trap allele dve^{1} (dve^{1}-*lacZ*) reflects the *dve-B* expression as well as GAL4 expression of NP1550 (Fig. S1A). Because the dve^{1}-*lacZ* expression was lost in $oc^{\gamma a1}$ mutant discs (Carr et al., 2005)(Figs. S1B, C), Dve-B is a major isoform expressed in the vertex region. Although the residual Dve protein expression in $oc^{\gamma a1}$ mutant discs may reflect Dve-A expression, homozygous mutants for the *dve-A* null mutant allele dve^{E181} showed normal morphology (Fig. S1D). Therefore, the *dve-B* activity seems to be crucial for head vertex development.

Dve is required for en activation through maintenance of hh expression

In early developmental stage, *otd* expression is induced by the combined action of Wg and Hh signaling pathways. Once Otd expression is initiated, a positive autoregulatory feedback loop maintains its subsequent expression (Blanco et al., 2009; Royet and Finkelstein, 1996)(Fig. 1E). Ectopic Dve induction in Otd-expressing clones prompted us to examine whether Dve induction is necessary for this feedback loop. In *dve* null mutant clones, Otd was normally expressed (Fig. 3A), indicating that the positive autoregulatory feedback loop of *otd* does not require the downstream target gene *dve*. If Otd-induced En expression is also maintained in *dve* mutant clones, Dve appears to function in parallel with the Otd-En pathway for ocelli formation. However, En expression was completely lost in *dve* mutant clones (Fig. S2A), suggesting that Dve is also required for En expression as an essential factor in the Otd-Dve-En pathway.

Royet and Finkelstein showed that En expression is induced in the most medial region where Hh is expressed, and also that the reduced level of Hh also leads to the loss of En expression (Royet and Finkelstein, 1995; Royet and Finkelstein, 1996). These reports suggest that the Hh signaling pathway directly activates the En expression in the medial vertex region. Furthermore, a recent report suggests that Otd is required to maintain *hh* expression (Blanco et al., 2009). Consistent with this notion, En

expression was maintained in small mutant clones for *otd* or *dve* (Figs. S2B, C), whereas it was completely lost in large mutant clones (Fig. 2F and Fig. S2A). Thus, we examined the effect of *dve* mutation on *hh-lacZ* expression. In *dve* null mutant clones, the *hh-lacZ* expression was greatly reduced compared to the surrounding wild-type cells (Fig. 3B). Thus, it is likely that Otd-mediated *hh* maintenance is largely dependent on the activity of a downstream effector, Dve, because Otd is normally expressed in *dve* mutant clones. However, *hh-lacZ* was still weakly expressed, presumably due to the presence of Otd in these clones. These results strongly suggest that Otd alone is insufficient for *hh* maintenance, and also that the cooperative action between Otd and Dve is required for maximal level of *hh* expression. Consistent with this notion, forced *otd* or *dve-B* expression could not induce ectopic *hh* expression outside the *hh*-expressing domain (Fig. S3A, B). However, forced *otd* expression resulted in coexpression of Otd and Dve (Fig. 2G and Fig. S3A), suggesting that some positional cues are prerequisite for *hh* induction in the medial vertex region. Taken together, these results indicate that coexpression of Otd and Dve is required for maintaining *hh* expression, but insufficient for *hh* induction.

To further confirm the Hh-dependent En activation, we generated clones that Hh signaling is blocked. Hh-responsive changes in gene expression are mediated by the zinc finger transcription factor Cubitus interruptus (Ci), which can generate activating or repressing forms: a full-length transcriptional activator form (Ci^{155}) or a C-terminally truncated transcriptional repressor form (Ci^{75}) (Lum and Beachy, 2004). In Ci^{75}-expressing clones, Hh signaling is blocked, and En expression was repressed in a cell-autonomous manner, whereas Dve expression was unaffected (Fig. 3C). Thus, the Ci^{75}-mediated repression of *en* is relieved by Hh signaling in the ocellar region. Taken together, these results indicate that an Otd downstream effector, Dve, is required for En expression through the maintenance of *hh* expression in the medial vertex region.

Transient *en* induction at 100 hr AEL in the *oc* mutant background (*oc^{1}; hsp70-en*) partially rescued the ocelliless phenotype, and mutant mosaic clones for *en* led to almost complete loss of ocellar triangle with an enlarged ocellus (Royet and Finkelstein, 1995; Wehn and Campbell, 2006). These reports suggest that En is required for establishment of the ocellar cuticle and for proper spacing of ocelli rather than establishment of ocelli precursors. In ocellar precursors, Ci^{155} is involved in *eya* activation, whereas relieving the Ci^{75}-mediated repression is required for photoreceptor

differentiation in the compound eye (Pappu et al., 2003). It is an intriguing possibility that Hh signaling effectors, Ci^{155} and Ci^{75}, are differently required for specification of ocelli precursors and the ocellar cuticle, respectively.

Differential requirement of Otd and Dve in the head vertex region

Both *wg* and *hh* are required for head vertex development and they are expressed in orbital and ocellar cuticles, respectively (Royet and Finkelstein, 1996). In early third larval instar (72-84 hr after egg laying; AEL), *wg* and *hh* are coexpressed in the head vertex primordium, Dve is expressed more broadly in a graded fashion as well as the Otd expression pattern with highest concentration in the medial region (Royet and Finkelstein, 1996; Fig. S4A). In late third larval instar (84-96 hr AEL), *wg* expression is separated from *hh*-expressing domain (Royet and Finkelstein, 1996; Fig. S4B). Because this separation depends on the Otd activity (Blanco et al., 2009), we examined whether the Otd-mediated repression of *wg* is regulated through the Dve activity. Interestingly, *wg* expression was not de-repressed even in large *dve* mutant clones (Fig. 4A and Figs. S4C, D), although Dve is involved in *wg* repression in other tissues (Nakagoshi et al., 2002). Thus, the Otd-mediated *wg* repression is independent of the Dve activity.

Recently, Wang et al. (2010) reported that Otd is required and sufficient to repress *eye gone* (*eyg*) expression, and also that Eyg is a major factor to suppress ocellar development (Wang et al., 2010). Ectopic *eyg* expression in the vertex region results in nearly complete loss of ocelli, repression of the retinal determination gene *eya*, loss of ocellar bristles, and significant extra interocellar bristles, while the mediolateral frons and the lateral features are not affected (Wang et al., 2010). Because these phenotypes are different from the *dve* mutant phenotype, transformation of the ocellar cuticle into the frons cuticle, the Otd-mediated repression of *eyg* also appears to be independent of the Dve activity. As expected, in *dve* mutant clones, Eyg expression was unaffected, although Dve has a potential to repress Eyg expression (Figs. 4A, B). Taken together, these results indicate that Otd, but not Dve, is required to repress *wg* and *eyg* in the vertex region, whereas Otd and Dve regulate *hh* and *en* in a linear pathway.

To further examine the relationship between Otd and Dve, we checked double mutant phenotypes. In *dve* null mutant heads with the oc^{1} background, we observed

oc^{1} mutant phenotypes: loss of ocellar identity and residual frons formation (Fig. 4C). This result indicates that the Otd activity is prerequisite for transformation into frons in the *dve* mutant background. In *dve* null mutant discs with the *oc*^{1} background, expression of Wg and Eyg were de-repressed in the vertex region and showed the *oc*^{1} mutant phenotypes (Figs. 4D-F). Taken together, these results indicate that Otd has at least three functions: (1) Dve-dependent ocellar specification (maintenance of late *hh* expression and Hh-induced *en* activation), (2) Dve-independent ocellar specification (repression of *wg* and *eyg*), and (3) establishment of the frons identity in the mediolateral region. The Otd-induced frons identity is a default state and is repressed by Otd-induced Dve in an incoherent feedforward loop (iFFL) in the medial region (see Discussion).

Dve-mediated ara repression is crucial for ocelli development

Iroquois-Complex (Iro-C) encodes three homeodomain proteins, Araucan (Ara), Caupolican (Caup), and Mirror (Mirr). The *Iro-C* genes are expressed in the dorsal region of the eye-antennal disc and act as dorsal selectors (Gómez-Skarmeta et al., 1996; McNeill et al., 1997). The sequence similarity between Ara and Caup and their essentially identical patterns of expression suggest that these proteins may functionally replace each other (Gómez-Skarmeta et al., 1996). Therefore, we checked the expression patterns of *Iro-C* genes using *ara-lacZ* and *mirr-lacZ*. In the dorsal head capsule (vertex) region, *ara* and *mirr* are differentially expressed; Dve and *mirr-lacZ* are coexpressed (Figs. 5A, B), and Dve and *ara-lacZ* are expressed in a non-overlapping manner (Figs. 5C, D) in both disc proper (DP) and peripodial epithelium (PE). In *otd* or *dve* null mutant clones, *ara-lacZ* was de-repressed in the vertex region (Fig. 5E and Fig. S2D), suggesting a mechanism that Dve-mediated *ara* repression is crucial for head vertex development. To further examine the relationship between Dve and Ara, we performed *ara* mis-expression in the head vertex (*NP1550>ara*), and the progeny resulted in ocelli loss or small ocelli associated with reduced size of the ocellar cuticle (Fig. 5F). Other developmental defects in the ocellar region, loss of ocellar and interocellar bristles, were also observed with variable frequencies. However, frons and orbital cuticles were nearly normal (Fig. 5F). In these discs that *ara* is ectopically expressed in the vertex region, Dve expression was

normally maintained, whereas expression of *hh-lacZ,* En, and Eya were substantially reduced (Figs. 5G-J and data not shown). These results are consistent with *dve* mutant phenotypes (Figs. 3B, 5K, and Fig. S2A), suggesting that Dve-mediated repression of *ara* is important for specification of the ocellar identity.

To confirm this notion, we knocked down the *dve* expression using RNA interference (RNAi). Reduction of *dve* expression (*NP1550>dve-IR*) or Hh signaling (*NP1550>Ci*^{75}) resulted in the same phenotype: ocelli loss associated with transformation of the ocellar cuticle into the frons cuticle (Figs. 6A, B). If Dve-mediated repression of *ara* is crucial for ocellar specification, *ara* mutations should rescue the *dve* RNAi phenotype. The *dve* RNAi in the *ara* mutant background (*ara*^{rF209}*/ ara*^{rF209}*)* resulted in ocellar cuticle formation with several interocellar bristles without affecting the expression of GAL4 driver NP1550 (Fig. 6C and data not shown). In the heteroallelic combination with a large deletion allele (*ara*^{rF209}*/ iro*^{DFM3}), the *dve* RNAi phenotype was significantly rescued. The ocellar triangle was restored nearly to the wild-type pattern (Fig. 6D), and three ocelli could be formed (Figs. 6D', E), although the bristle patterning was still disorganized. Taken together, these results indicate that the Dve-mediated *ara* repression is crucial for ocellar specification.

Partial rescue of oc mutant phenotype by dve-B expression

As *dve* RNAi phenotype was significantly rescued in the *ara* mutant background, we examined whether the Dve-mediated *ara* repression is sufficient to rescue the *oc* mutant phenotype. Although NP1550 is a good GAL4 driver line to induce vertex expression, the GAL4 expression depends on the *dve-B* enhancer activity (Fig. S1), and its expression is greatly reduced in the *oc* mutant background (data not shown). Therefore, we used the NP4065 line whose GAL4 activity is detected in the vertex region (Wang et al., 2010). Hemizygous males for the recombinant chromosome *NP4065 oc*^{1} showed the greatly reduced Otd expression and completely lost the En expression in the medial vertex region of the eye-antennal disc (Fig. 7A). The hemizygous male (*NP4065 oc*^{1}*/ Y*) showed the *oc* mutant phenotypes in the adult head: loss of ocellar and frons cuticles (Fig. 7B). Transient *dve-B* induction at the mid-late third larval instar in this mutant background partially rescued the *oc* mutant phenotype. The rescued adult heads had very small lateral ocelli (Fig. 7C, arrows), although the

arrangement of frons cuticle and the bristle patterning were still irregular. Taken together, these rescue experiments clearly show the regulatory pathway of Otd-Dve-Ara.

Discussion

In this study, we present evidence that Dve is a new member involved in ocellar specification and acts as a downstream effector of Otd. Our results also revealed a complicated pathway of transcriptional regulators, Otd-Dve-Ara-Ci-En, for ocellar specification (Fig. 8A).

Dve-mediated transcriptional repression in coherent feedforward loops

Transcription networks contain a small set of recurring regulation patterns called network motifs. A feedforward loop (FFL) consists of three genes, two input transcription factors and a target gene, and their regulatory interactions generate eight possible structures of FFL (Alon, 2007; Mangan and Alon, 2003). When a target gene is suppressed by a repressor 1 (Rep1), relief of this repression by another repressor 2 (Rep2) can induce the target gene expression. When Rep2 also acts as an activator of the target gene, this relief of repression mechanism is classified as a coherent type-4 feedforward loop (c-FFL) (Alon, 2007; Mangan and Alon, 2003; Fig. 8B). During vertex development, Ara is involved in *hh* repression, and the Dve-mediated *ara* repression is crucial for *hh* expression and subsequent ocellar specification. However, the cascade of *dve-ara-hh* seems to be a relief of repression rather than a cFFL, because Dve is not a direct activator of the *hh* gene. Furthermore, *dve* RNAi phenotypes were rescued in the *ara* mutant background (Figs. 6C-E), suggesting that a linear relief of repression mechanism is crucial for *hh* maintenance.

In photoreceptor R7, Dve acts as a key molecule in a cFFL. Dve (as a Rep1) represses *rh3*, and the transcription factor Spalt (Sal) (as a Rep2) represses *dve* and also activates *rh3* in parallel to induce *rh3* expression (Johnston et al., 2011; Fig. 8D). Interestingly, Notch signaling is closely associated with the relief of Dve-mediated transcriptional repression in wing and leg discs. These regulatory networks may also be cFFLs in which Dve acts as a Rep1, although repressors involved in *dve* repression are not yet identified. In wing discs, expression of *wg* and *ct* are repressed by Dve,

and Notch signaling represses *dve* to induce these genes at the dorso-ventral boundary (Kölzer et al., 2003; Nakagoshi et al., 2002). The Dve activity adjacent to the dorso-ventral boundary still represses *wg* to refine the source of morphogen (Nakagoshi et al., 2002). In leg discs, Dve represses expression of *dAP-2*, and Notch signaling represses *dve* to induce *dAP-2* at the presumptive joint region. The Dve activity distal to the segment boundary still represses *dAP-2* to prevent ectopic joint formation (Shirai et al., 2007). Taken together, these results suggest that Dve plays a critical role as a Rep1 in cFFLs in different tissues. In the head vertex region, it is likely that the repressor activity of Dve is repressed in a cFFL to induce frons identity (see below).

Incoherent feedforward loops of Otd and Dve finely specify cell fates

The homeodomain protein Otd is the most upstream transcription factor required for establishment of the head vertex. During second larval instar, Otd is ubiquitously expressed in the eye-antennal disc and it is gradually restricted in the vertex primordium until early third larval instar (Royet and Finkelstein, 1995). Expression of an Otd-target gene, *dve*, is also detected in the same vertex region at early third larval instar. Otd is required for Dve expression, and the Otd-induced Dve is required for repression of frons identity through the Hh signaling pathway in the medial region. However, Otd is also required for the frons identity in both the medial and mediolateral regions (Fig. 8A).

This regulatory network is quite similar to the incoherent type-1 feedforward loop (iFFL) in photoreceptor R7. Otd-induced Dve is involved in *rh3* repression, whereas Otd is also required for *rh3* activation (Johnston et al., 2011; Figs. 8C, D). iFFLs have been known to generate pulse-like dynamics and response acceleration if Rep1 does not completely represses its target gene expression (Alon, 2007). However, the repressor activity of Dve supersedes the Otd-dependent *rh3* activation, resulting in complete *rh3* repression in yR7. In pR7, Dve is repressed by Sal, resulting in *rh3* expression through the Otd- and Sal-dependent *rh3* activation. Thus, Dve serves as a common node that integrates the two loops, the Otd-Dve-Rh3 iFFL and the Sal-Dve-Rh3 cFFL (Johnston et al., 2011; Fig. 8D).

In the head vertex region, Otd and Dve are expressed in a graded fashion along the mediolateral axis with highest concentration in the medial region (Royet and Finkelstein,

1996; Fig. S4A). It is assumed that Otd determines the default state for frons development through restricting the source of morphogens Hh and Wg, and also that high level of Dve expression in the medial ocellar region represses the frons identity through an iFFL (Fig. 8E). It is likely that repression of *dve* by an unknown repressor X occurs in a cFFL and induces the frons identity in the mediolateral region.

Interlocked loops of Dve-mediated transcriptional repression

Interlocked FFLs including Otd and Dve appear to be a common feature in the eye and the head vertex. However, other factors are not shared between two tissues. In R7, a default state is the Otd-dependent Rh3 activation, an acquired state is (1) Rh3 repression through the Otd-Dve iFFL and (2) Spineless-dependent Rh4 expression (Wernet et al., 2006). In the vertex, a default state is Otd-dependent frons formation, an acquired state is (1) frons repression through the Otd-Dve iFFL and (2) Hh-dependent ocellar specification associated with En and Eya activation.

Both Otd and Dve are K50-type homeodomain transcription factors, and they bind to the *rh3* promoter via canonical K50 binding sites (TAATCC) (Johnston et al., 2011; Tahayato et al., 2003). The Otd-Dve iFFL in the eye depends on direct binding activities to these K50 binding sites, but the iFFL in the vertex seems to be more complex. Although target genes for frons determination are not identified, the iFFL in the vertex includes some additional network motifs (Fig. 8A). For instance, in the downstream of Dve, Hh signaling is critically required for repression of the frons identity.

Since iFFLs also act as fold-change detection to normalize noise in inputs (Goentoro et al., 2009), interlocked FFLs of Dve-mediated transcriptional repression may contribute to robustness of gene expression by preventing aberrant activation. It is an intriguing possibility that, in wing and leg discs, Dve also serves as a common node that integrates the two loops as observed in the eye and the vertex. Further characterization of regulatory networks including Dve will clarify molecular mechanisms of cell specification.

Acknowledgments

We are grateful to A. Singh, Y. H. Sun, N. Azpiazu, S. Ishii, T. Kojima, J. Modolell, the Bloomington Stock Center, and the Drosophila Genetic Resource Center (DGRC, Kyoto) for fly strains and antibodies; C. Desplan, R. Johnston, A. Singh, T. Kojima, and T. Adachi-Yamada for helpful discussion; A. Singh for comments on the manuscript. We also thank the Advanced Science Research Center (Okayama University) for the use of confocal microscope OLYMPUS FV300. This work was partially supported by Grant-in-Aid from the Ministry of Education, Culture, Sports, Science and Technology (to H. N.).

References

Aldaz, S., Morata, G., Azpiazu, N., 2003. The Pax-homeobox gene *eyegone* is involved in the subdivision of the thorax of *Drosophila*. *Development* **130,** 4473-4482.

Alon, U., 2007. Network motifs: theory and experimental approaches. *Nat. Rev. Genet.* **8,** 450-461.

Aza-Blanc, P., Ramirez-Weber, F.A., Laget, M.P., Schwartz, C., Kornberg, T.B., 1997. Proteolysis that is inhibited by *hedgehog* targets Cubitus interruptus protein to the nucleus and converts it to a repressor. *Cell* **89,** 1043-1053.

Blanco, J., Seimiya, M., Pauli, T., Reichert, H., Gehring, W.J., 2009. Wingless and Hedgehog signaling pathways regulate *orthodenticle* and *eyes absent* during ocelli development in *Drosophila*. *Dev. Biol.* **329,** 104-115.

Carr, M., Hurley, I., Fowler, K., Pomiankowski, A., Smith, H.K., 2005. Expression of *defective proventriculus* during head capsule development is conserved in *Drosophila* and stalk-eyed flies (*Diopsidae*). *Dev. Genes Evol.* **215,** 402-409.

Chen, Y., Gallaher, N., Goodman, R.H., Smolik, S.M., 1998. Protein kinase A directly regulates the activity and proteolysis of cubitus interruptus. *Proc. Natl. Acad. Sci. U. S. A.* **95,** 2349-2354.

Cohen, S., Jurgens, G., 1991. *Drosophila* headlines. *Trends Genet.* **7,** 267-272.

Finkelstein, R., Perrimon, N., 1991. The molecular genetics of head development in *Drosophila* melanogaster. *Development* **112,** 899-912.

Finkelstein, R., Smouse, D., Capaci, T.M., Spradling, A.C., Perrimon, N., 1990. The *orthodenticle* gene encodes a novel homeo domain protein involved in the

development of the *Drosophila* nervous system and ocellar visual structures. *Genes Dev.* **4,** 1516-1527.

Goentoro, L., Shoval, O., Kirschner, M.W., Alon, U., 2009. The incoherent feedforward loop can provide fold-change detection in gene regulation. *Mol. Cell* **36,** 894-899.

Gómez-Skarmeta, J.L., Diez del Corral, R., de la Calle-Mustienes, E., Ferre-Marco, D., Modolell, J., 1996. Araucan and caupolican, two members of the novel iroquois complex, encode homeoproteins that control proneural and vein-forming genes. *Cell* **85,** 95-105.

Hartenstein, V., Jan, Y.N., 1992. Studying *Drosophila* embryogenesis with P-lacZ enhancer trap lines. *Roux's Arch. Dev. Biol.* **201,** 194-220.

Hayashi, S., Ito, K., Sado, Y., Taniguchi, M., Akimoto, A., Takeuchi, H., Aigaki, T., Matsuzaki, F., Nakagoshi, H., Tanimura, T., Ueda, R., Uemura, T., Yoshihara, M., Goto, S., 2002. GETDB, a database compiling expression patterns and molecular locations of a collection of Gal4 enhancer traps. *Genesis* **34,** 58-61.

Haynie, J.L., Bryant, P.J., 1986. Development of the eye-antenna imaginal disc and morphogenesis of the adult head in *Drosophila melanogaster*. *J. Exp. Zool.* **237,** 293-308.

Ito, K., Awano, W., Suzuki, K., Hiromi, Y., Yamamoto, D., 1997. The *Drosophila* mushroom body is a quadruple structure of clonal units each of which contains a virtually identical set of neurones and glial cells. *Development* **124,** 761-771.

Johnston, R.J., Otake, Y., Sood, P., Vogt, N., Behina, R., Vasiliauskas, D., McDonald, E., Xie, B., Koenig, S., Wolf, R., Cook, T., Gebelein, B., Kussell, E., Nakagoshi, H., Desplan, C., 2011. Interlocked feedforward loops control Rhodopsin expression in the *Drosophila* eye. *Cell*, (in press).

Jurgens, G., Hartenstein, V., 1993. The terminal regions of the body pattern, in: Bate, M. and Martinez Arias, A. (Eds.), The development of *Drosophila melanogaster*. Cold Spring Harbor Laboratory Press, Cold Spring Harbor, pp. 687-746.

Kassis, J.A., Noll, E., VanSickle, E.P., Odenwald, W.F., Perrimon, N., 1992. Altering the insertional specificity of a *Drosophila* transposable element. *Proc. Natl. Acad. Sci. U. S. A.* **89,** 1919-1923.

Kenyon, K.L., Ranade, S.S., Curtiss, J., Mlodzik, M., Pignoni, F., 2003. Coordinating proliferation and tissue specification to promote regional identity in the

Drosophila head. *Dev. Cell* **5,** 403-414.

Kölzer, S., Fuss, B., Hoch, M., Klein, T., 2003. *defective proventriculus* is required for pattern formation along the proximodistal axis, cell proliferation and formation of veins in the *Drosophila* wing. *Development* **130,** 4135-4147.

Lee, T., Luo, L., 1999. Mosaic analysis with a repressible cell marker for studies of gene function in neuronal morphogenesis. *Neuron* **22,** 451-461.

Lum, L., Beachy, P.A., 2004. The Hedgehog response network: sensors, switches, and routers. *Science* **304,** 1755-1759.

Mangan, S., Alon, U., 2003. Structure and function of the feed-forward loop network motif. *Proc. Natl. Acad. Sci. USA* **100,** 11980-11985.

McNeill, H., Yang, C.H., Brodsky, M., Ungos, J., Simon, M.A., 1997. *mirror* encodes a novel PBX-class homeoprotein that functions in the definition of the dorsal-ventral border in the *Drosophila* eye. *Genes Dev.* **11,** 1073-1082.

Nakagawa, Y., Fujiwara-Fukuta, S., Yorimitsu, T., Tanaka, S., Minami, R., Shimooka, L., Nakagoshi, H., 2011. Spatial and temporal requirement of Defective proventriculus activity during *Drosophila* midgut development. *Mech. Dev.*, (in press).

Nakagoshi, H., Hoshi, M., Nabeshima, Y., Matsuzaki, F., 1998. A novel homeobox gene mediates the Dpp signal to establish functional specificity within target cells. *Genes Dev.* **12,** 2724-2734.

Nakagoshi, H., Shirai, T., Nabeshima, Y., Matsuzaki, F., 2002. Refinement of *wingless* expression by a Wingless- and Notch-responsive homeodomain protein, Defective proventriculus. *Dev. Biol.* **249,** 44-56.

Newsome, T.P., Asling, B., Dickson, B.J., 2000. Analysis of *Drosophila* photoreceptor axon guidance in eye-specific mosaics. *Development* **127,** 851-860.

Pappu, K.S., Chen, R., Middlebrooks, B.W., Woo, C., Heberlein, U., Mardon, G., 2003. Mechanism of hedgehog signaling during *Drosophila* eye development. *Development* **130,** 3053-3062.

Punzo, C., Seimiya, M., Flister, S., Gehring, W.J., Plaza, S., 2002. Differential interactions of *eyeless* and *twin of eyeless* with the *sine oculis* enhancer. *Development* **129,** 625-634.

Royet, J., Finkelstein, R., 1995. Pattern formation in *Drosophila* head development: the role of the *orthodenticle* homeobox gene. *Development* **121,** 3561-3572.

Royet, J., Finkelstein, R., 1996. *hedgehog, wingless* and *orthodenticle* specify adult head development in *Drosophila*. *Development* **122,** 1849-1858.

Royet, J., Finkelstein, R., 1997. Establishing primordia in the *Drosophila* eye-antennal imaginal disc: the roles of *decapentaplegic, wingless* and *hedgehog*. *Development* **124,** 4793-4800.

Shirai, T., Maehara, A., Kiritooshi, N., Matsuzaki, F., Handa, H., Nakagoshi, H., 2003. Differential requirement of EGFR signaling for the expression of *defective proventriculus* gene in the *Drosophila* endoderm and ectoderm. *Biochem. Biophys. Res. Commun.* **311,** 473-477.

Shirai, T., Yorimitsu, T., Kiritooshi, N., Matsuzaki, F., Nakagoshi, H., 2007. Notch signaling relieves the joint-suppressive activity of Defective proventriculus in the Drosophila leg. *Dev. Biol.* **312,** 147-156.

Tahayato, A., Sonneville, R., Pichaud, F., Wernet, M.F., Papatsenko, D., Beaufils, P., Cook, T., Desplan, C., 2003. Otd/Crx, a dual regulator for the specification of ommatidia subtypes in the Drosophila retina. *Dev. Cell* **5,** 391-402.

Terriente, J., Perea, D., Suzanne, M., Diaz-Benjumea, F.J., 2008. The *Drosophila* gene *zfh2* is required to establish proximal-distal domains in the wing disc. *Dev. Biol.* **320,** 102-112.

Wang, L.H., Huang, Y.T., Tsai, Y.C., Sun, Y.H., 2010. The role of *eyg* Pax gene in the development of the head vertex in *Drosophila*. *Dev. Biol.* **337,** 246-258.

Wehn, A., Campbell, G., 2006. Genetic interactions among *scribbler, Atrophin* and *groucho* in *Drosophila* uncover links in transcriptional repression. *Genetics* **173,** 849-861.

Wernet, M.F., Mazzoni, E.O., Celik, A., Duncan, D.M., Duncan, I., Desplan, C., 2006. Stochastic *spineless* expression creates the retinal mosaic for colour vision. *Nature* **440,** 174-180.

Xu, T., Rubin, G.M., 1993. Analysis of genetic mosaics in developing and adult *Drosophila* tissues. *Development* **117,** 1223-1237.

Figure legends

Fig. 1 *dve* mutant phenotypes in the ocellar region

(A) A dorsal head capsule (vertex) of wild-type (WT) adult head. The most medial triangular cuticle is the ocellar region, which contains three ocelli. The mediolateral subdomain (frons) shows ridged cuticle and has no bristle. The lateral subdomain (orbital cuticle) occupies the space between the frons and the compound eyes, and has a stereotypical array of macrochaetes. (B) A *dve* null mutant mosaic head (*y w hs-flp/ Y; FRT42D* dve^{L186}*/ ey-FLP5 FRT42D ubi-GFP[*w^{+}*] M(2)53*^{1}). The ocellar cuticle is transformed into the frons cuticle. (C) An *ocelliless* (*oc*) mutant head (oc^{ya1}*/ Y*). Both the ridged cuticle of frons and structures of the ocellar cuticle are lost. (D) A weak *oc* mutant head (oc^{1}*/ Y*). The frons cuticle partially remains (arrows). (E) Regulatory pathways for ocelli development. The Otd target genes *hh*, *en*, and *eya* are required for ocelli formation together with *sine oculis* (*so)*. L3: third-larval instar.

Fig. 2 Otd is sufficient for *dve* induction but not for *en*

(A) dve^{NP1550}*-GAL4*-driven GFP expression (*NP1550>GFP*, green) nearly reflects the endogenous Dve expression (magenta) in the vertex region. (B) Otd expression (magenta) is nearly identical to that of *NP1550>GFP* (green). (C, C') Dve (magenta) and En (green) is coexpressed in the head vertex primordium in a wild-type eye-antennal disc (arrows). (D) In weak oc^{1} mutant discs, Dve expression is reduced. (E) In strong oc^{ya1} mutant discs, Dve protein expression is greatly reduced in the vertex region. (D', E') En expression is completely lost in the vertex region in *oc* mutant discs. (F-F") Expression of Dve (blue, F') and En (red, F") in *otd* mutant clones (green, positively labeled with GFP) generated with the MARCM system (*w* otd^{YH13} *FRT19A/tub-GAL80 hs-FLP FRT19A; ey-flp5/UAS-mCD8::GFP; tub-GAL4/+*). Both Dve and En expression are completely lost within a large *otd* mutant clone. (G-G") Effects of forced *otd* expression with the Ay-GAL4 system. In an Otd-expressing clone (green, positively labeled with GFP) outside the vertex region, Dve is ectopically induced (arrowheads) in a cell-autonomous manner, whereas En is not induced (G").

Fig.3 Dve is required for maintenance of *hh* expression in the vertex region
(A-A") Otd expression (magenta) is unaffected in *dve* null mutant clones marked by the absence of GFP expression (*y w ey-flp2/ Y; FRT42D dve^{L186}/ FRT42D ubi-GFP[w^{+}]*). (B-B") Expression of *hh-lacZ* (red) is substantially reduced in a *dve* null mutant clone marked by the absence of GFP expression (*y w ey-flp2/ Y; FRT42D dve^{L186}/ FRT42D ubi-GFP[w^{+}]; hh-lacZ/+*). (C-C") Inhibition of the Hh signaling pathway with the Ay-GAL4 system. In Ci^{75}-expressing clones (green, positively labeled with GFP) within the vertex region, En expression (red) is lost in a cell-autonomous manner (C'), whereas Dve expression (blue) is unaffected (C").

Fig. 4 Differential requirement of Otd and Dve in the head vertex region
(A-A") Expression of Eyg (red) and Wg (blue) are unaffected in *dve* null mutant clones marked by the absence of GFP expression (*y w ey-flp2/ Y; FRT42D dve^{L186}/ FRT42D ubi-GFP[w^{+}]*). (B) Forced *dve-B* expression with the Ay-GAL4 system (*Ay>dve-B*). In Dve-B-expressing clones (green, positively labeled with GFP), Eyg expression is completely lost. (C) An *oc^{1} dve^{L186}* double mutant head shows loss of ocellar identity and residual frons formation (*ct oc^{1}/Y FRT42D dve^{L186}/ eyFLP5 FRT42D ubi-GFP[w^{+}] M(2)53^{1}*). (D-D") A heterozygous *oc^{1}* disc (*oc^{1}/ FM7GFP*) shows normal expression patterns of Eyg and Wg. Eyg is expressed in an anterior-dorsal stripe and excluded from the head vertex primordium (D') and the expression domains of Wg are restricted to two lateral patches (D"). They are not detected in the vertex region (arrows). (E-E") In hemizygous *oc^{1}* discs (*oc^{1}/Y*), Eyg expression expands into the vertex region (arrowhead in E') and Wg expression fails to disappear from the medial region (arrowhead in E"). (F-F") In *oc^{1} dve^{L186}* double mutant discs, the expression patterns of Eyg and Wg (arrowheads) are similar to those in *oc^{1}* discs.

Fig. 5 Ara represses ocellar development
(A, B) *mirr-lacZ* is expressed in the dorsal half of the eye disc in the disc proper (DP) layer (A) and in all dorsal half region of the peripodial epithelium (PE) layer (B). Co-expression of Dve and *mirr-lacZ* in white is evident in the vertex region (arrowheads). (C, D) *ara-lacZ* is expressed in the dorsal half of the eye disc in the DP layer (C). It is expressed in the dorso-posterior region and on the DV midline of the eye-antennal PE layer (D). Expression of Dve and *ara-lacZ* are non-overlapping in

both layers. (E-E") In *dve* null mutant clones, *ara-lacZ* (red) is ectopically expressed in the vertex region (arrowhead in E'). Adjacent to the mutant clone, ectopic *ara-lacZ* expression is also induced in a cell non-autonomous manner (arrow in E'). (F) Forced expression of *ara* in the vertex region (*NP1550>ara*) results in ocelli loss or small ocelli associated with reduced size of the ocellar cuticle, while frons and orbital cuticles are nearly normal. (G-K) Expression patterns of *hh-lacZ* (G, H) and the ocelli precursor marker Eya (I-K) in discs of control (G, I), *NP1550>ara* (H and J), and *dve* null mutant clones (K). Expression of *hh-lacZ* (H) and Eya (J) are greatly reduced in *NP1550>ara*, and only a cluster of weak Eya expression is observed (arrowhead in J). Expression of Eya (magenta in K) is completely lost in *dve* null mutant clones marked by the absence of GFP expression (*y w hs-flp/ Y; FRT42D* dve^{L186}*/ ey-FLP5 FRT42D ubi-GFP[*w^{+}*] M(2)53*^{1}).

Fig. 6 *dve* knockdown phenotype is rescued in the *ara* mutant background
(A) RNAi induction for *dve* mRNA in the vertex region (*NP1550>dve-IR*) induces the slightly mild *dve* mutant phenotypes. (B) Forced expression of Ci^{75} (*NP1550>*Ci^{75}) induces the *hh* mutant phenotype: transformation of ocellar cuticle into frons. (C) *dve* RNAi in the *ara* homozygous background (*NP1550/UAS-dve-IR;* ara^{rF209}) results in ocellar cuticle formation with several interocellar bristles. (D, E) *dve* RNAi in the *ara* heteroallelic combination background (*NP1550/UAS-dve-IR;* ara^{rF209}*/* iro^{DFM3}) results in formation of the ocellar cuticle (D), and three ocelli (arrowheads in D', E). The white arrowhead in D' shows a very small ocellus. Two images in D and D' are obtained from the same fly.

Fig. 7 Partial rescue of *oc* mutant phenotype by *dve-B* expression
(A) Expression pattern of NP4065 in the oc^{1} mutant background (*NP4065* oc^{1}*>GFP*). The NP4065-driven GFP signal (green) is detected in the medial region of the vertex (arrowhead in A) in which Otd (blue) and En (red) expression are lost. (B) An adult head of hemizygous *NP4065* oc^{1} male reared at 18°C (*NP4065* oc^{1}*/Y*) shows the oc^{1} mutant phenotype. (C, C') An oc^{1} adult head rescued by transient *dve-B* expression (*NP4065* oc^{1}*/Y; UAS-dve-B/+;* $tub\text{-}GAL80^{ts}$*/+*). Two lateral ocelli are partially formed (arrows), however, the arrangement of frons cuticle and bristle patterning are still irregular.

Fig. 8　Schematic representation for cell specification in the head and the eye.
(A) Regulatory networks for vertex specification.　Otd activates *dve* expression, and the Otd-induced Dve maintains late *hh* expression as a linear pathway (broken arrows) through the relief of repression by Ara/Caup.　Factors required for ocellar specification (*dve*, *hh*, Ci^{155}, *eya*, and *en*) and the ocellar region (cuticle and ocelli) are shown in magenta.　The Otd activity is required for frons identity (gray), whereas Otd- and Dve-mediated Hh signaling also represses the frons development.　The Dve-independent Otd activities, positive autoregulatory feedback and the relief of repression by Wg and Eyg are shown in blue.　(B) A coherent type-4 feedforward loop (cFFL).　(C) An incoherent type-1 feedforward loop (iFFL).　(D) Interlocked feedforward loops in photoreceptor cells (Johnston et al., 2011).　Otd is required for *rh3* expression, whereas Otd also activates the *rh3* repressor Dve in yellow-type R7 (yR7) to lead *rh3* repression in an iFFL (magenta).　In pale-type R7 (pR7), Spalt (Sal) represses *dve* and induces *rh3* expression in a cFFL.　(E) The feedforward loops of Otd and Dve in the vertex region.　Dve is a putative repressor 1 (Rep 1) that represses frons determinant gene(s), and unknown factor X should act as a repressor 2 (Rep 2) to repress *dve* and also to induce frons identity in a cFFL.

Figure legends for supplementary figures

Fig. S1 Expression of the type-B isoform (*dve-B*) in the vertex region

(A) Organization of the *dve* locus. The type-B specific exon 2B is indicated by blue. The reporter gene expression of the enhancer-trap allele dve^{1} and the GAL4 enhancer-trap line NP1550 reflect the *dve-B* expression. dve^{E181} is a type-A null allele that completely removes the first exon for the type-A (*dve-A*) transcript. (B) In late third larval instar, dve^{1}*-lacZ* (green) is expressed in the entire vertex region as the same expression pattern for Dve protein (magenta). (C) In oc^{ya1} mutant discs, Dve protein expression (magenta) is greatly reduced in the vertex region. Expression of dve^{1}*-lacZ* (green) is almost completely lost. (D) A dve^{E181} homozygous mutant head. No morphological abnormality is observed in the *dve-A* null mutant head.

Fig. S2 En activation by Otd and Dve is indirectly regulated.

(A and A') In large *dve* mutant clones marked by the absence of GFP expression (*y w hs-flp/ y w; FRT42D* dve^{L186}*/ ey-flp5 FRT42D ubi-GFP[*w^{+}*] M(2)53*^{1}), En expression (magenta) in the vertex region is completely lost (arrow in A'). (B-B") In a small *dve* null mutant clone marked by the absence of GFP expression (*y w ey-flp2/ Y; FRT42D* dve^{L186}*/ FRT42D ubi-GFP[*w^{+}*]*), En expression (magenta) is maintained (arrowheads). (C-C") In an *otd* null mutant clone (green, positively labeled with GFP) generated with the MARCM system (oc^{2} *FRT19A/ w tubP-GAL80 hsFLP FRT19A; ey-flp5/ UAS-mCD8::GFP; tubP-GAL4*/+), Dve expression is completely lost in a cell-autonomous manner (C'), whereas En expression is only partially reduced (C"). (D-D") *ara-lacZ* is ectopically expressed in *otd* null mutant clone as observed in *dve* mutant clones (oc^{2} *FRT19A/ w tubP-GAL80 hsFLP FRT19A; ey-flp5/ UAS-mCD8::GFP; tubP-GAL4*/*ara-lacZ*).

Fig. S3 Forced expression of a factor required for En activation

(A, B) Forced expression of *otd* (A) or *dve-B* (B) with the Ay-GAL4 system (*Ay>otd* or *Ay>dve-B*). In Otd-expressing clones (green in A, positively labeled with GFP) outside the vertex region, Dve (blue) is ectopically induced in a cell-autonomous manner (arrowheads), whereas *hh-lacZ* (red) is not induced. In Dve-B-expressing clones (green in B, positively labeled with GFP), *hh-lacZ* (red) is not induced outside

the vertex region. (C) Activation of the Hh signaling pathway with the Ay-GAL4 system (Ay>Ci^{155}). In Ci^{155}-expressing clones (green, positively labeled with GFP), Dve (blue) and En expression (red) are unaffected.

Fig. S4 Dve and Wg expression patterns in the vertex region

(A-A") In the early third larval instar, Hh signaling (*ptc>GFP*, green) is active in cells that express *wg-lacZ* (red). Dve expression (blue) is more broadly detected in a graded fashion with highest concentration in the medial region. Arrows indicate the lowest expression in the lateral region. (B-B") In the late third larval instar, two *wg*-expressing domains (red) are separated from *ptc>GFP*-expressing domain (green). Dve expression (blue) is detected in the entire vertex region. Dve-expressing region includes cells that Hh signaling is active, and partly overlaps with *wg*-expressing cells. (C, D) Expression of *wg-lacZ* (magenta) in control discs (C; *y w hs-flp/ Y; wg-lacZ FRT42D dve^{E38}*/+) and in large *dve* mutant clones (D; *y w hs-flp/ Y; wg-lacZ FRT42D dve^{E38}/ ey-FLP5 FRT42D ubi-GFP[w^{+}] M(2)53^{1}*). Dve expression is shown in green (C), and *dve* mutant clones are marked by the absence of GFP expression (green in D).

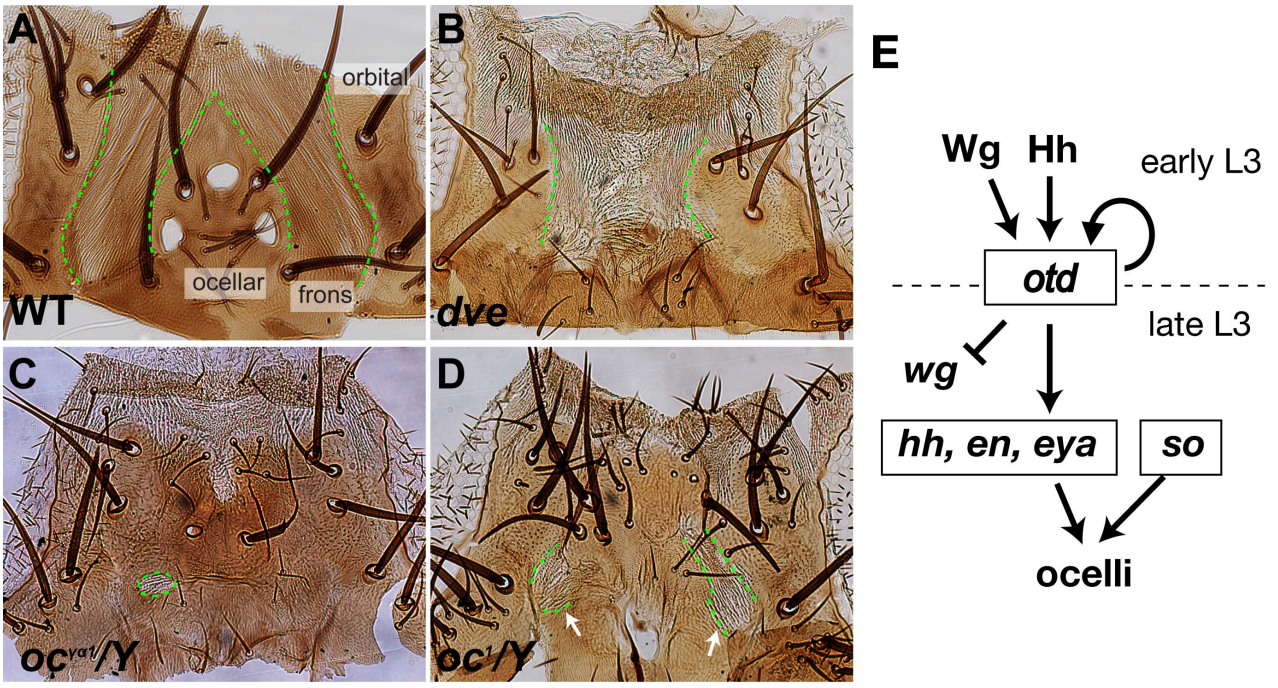
A
orbital
ocellar
frons
WT
B
dve
C
D
E
Wg
Hh
early L3
otd
late L3
wg
hh, en, eya
so
ocelli

Fig. 1

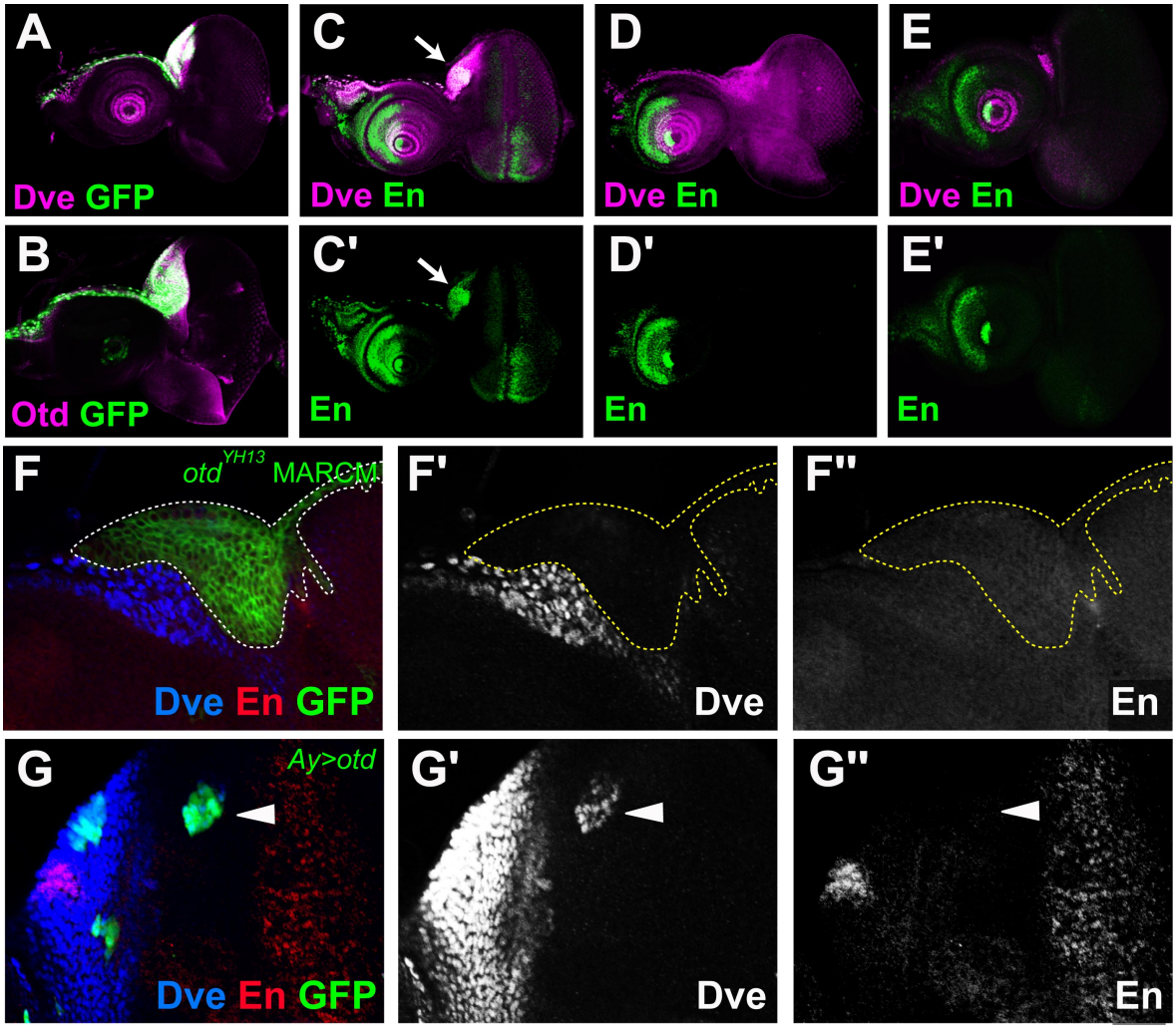
A
Dve GFP
C
Dve En
D
Dve En
E
Dve En
B
Otd GFP
C'
En
D'
En
E'
En
F
otd YH13 MARCM
Dve En GFP
F'
Dve
F''
En
G
Ay>otd
Dve En GFP
G'
Dve
G''
En

Fig. 2

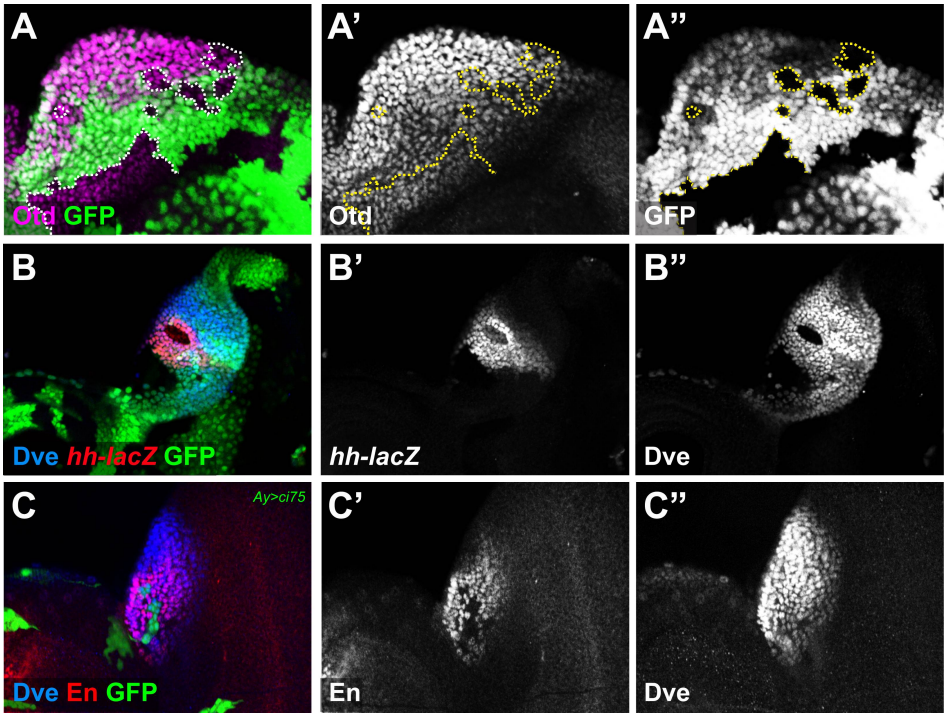
A
Otd GFP
A'
Otd
A''
GFP
B
Dve hh-lacZ GFP
B'
hh-lacZ
B''
Dve
C
Ay>ci75
Dve En GFP
C'
En
C''
Dve

Fig. 3

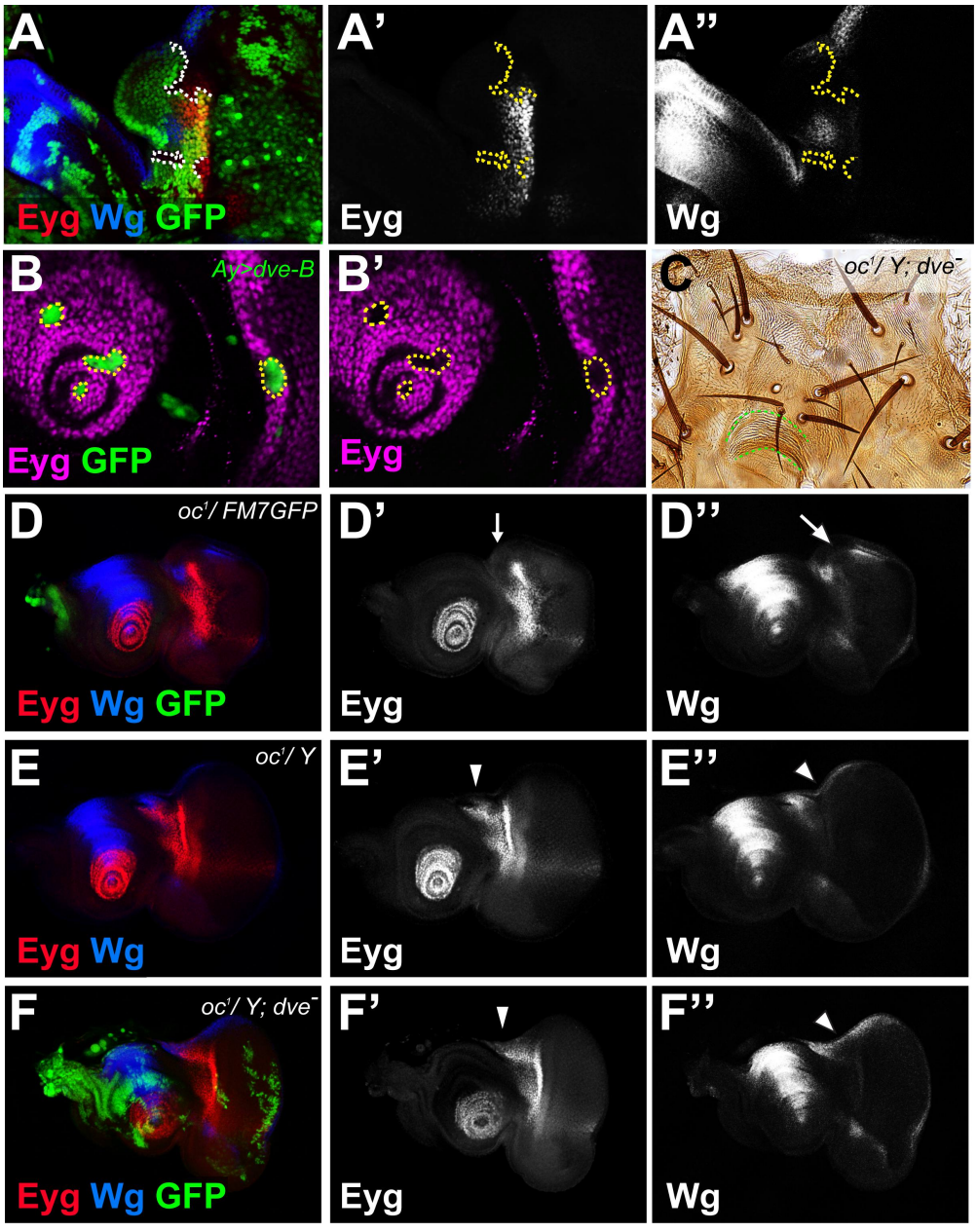
A
Eyg Wg GFP
A'
Eyg
A''
Wg
B
Ay>dve-B
Eyg GFP
B'
Eyg
C
oc¹/ Y; dve⁻
D
oc¹/ FM7GFP
Eyg Wg GFP
D'
Eyg
D''
Wg
E
oc¹/ Y
Eyg Wg
E'
Eyg
E''
Wg
F
oc¹/ Y; dve⁻
Eyg Wg GFP
F'
Eyg
F''
Wg

Fig. 4

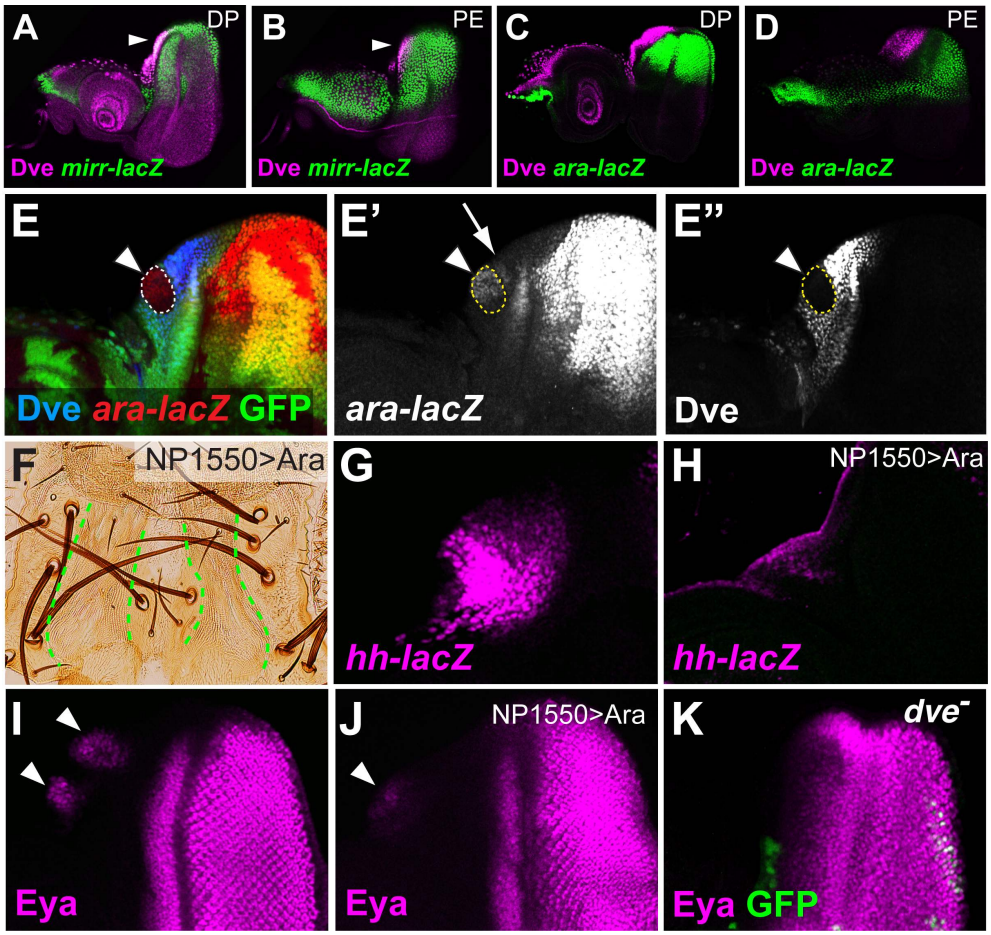
A
DP
Dve mirr-lacZ
B
PE
Dve mirr-lacZ
C
DP
Dve ara-lacZ
D
PE
Dve ara-lacZ
E
Dve ara-lacZ GFP
E'
ara-lacZ
E''
Dve
F
NP1550>Ara
G
hh-lacZ
H
NP1550>Ara
hh-lacZ
I
Eya
J
NP1550>Ara
Eya
K
dve-
Eya GFP

Fig. 5

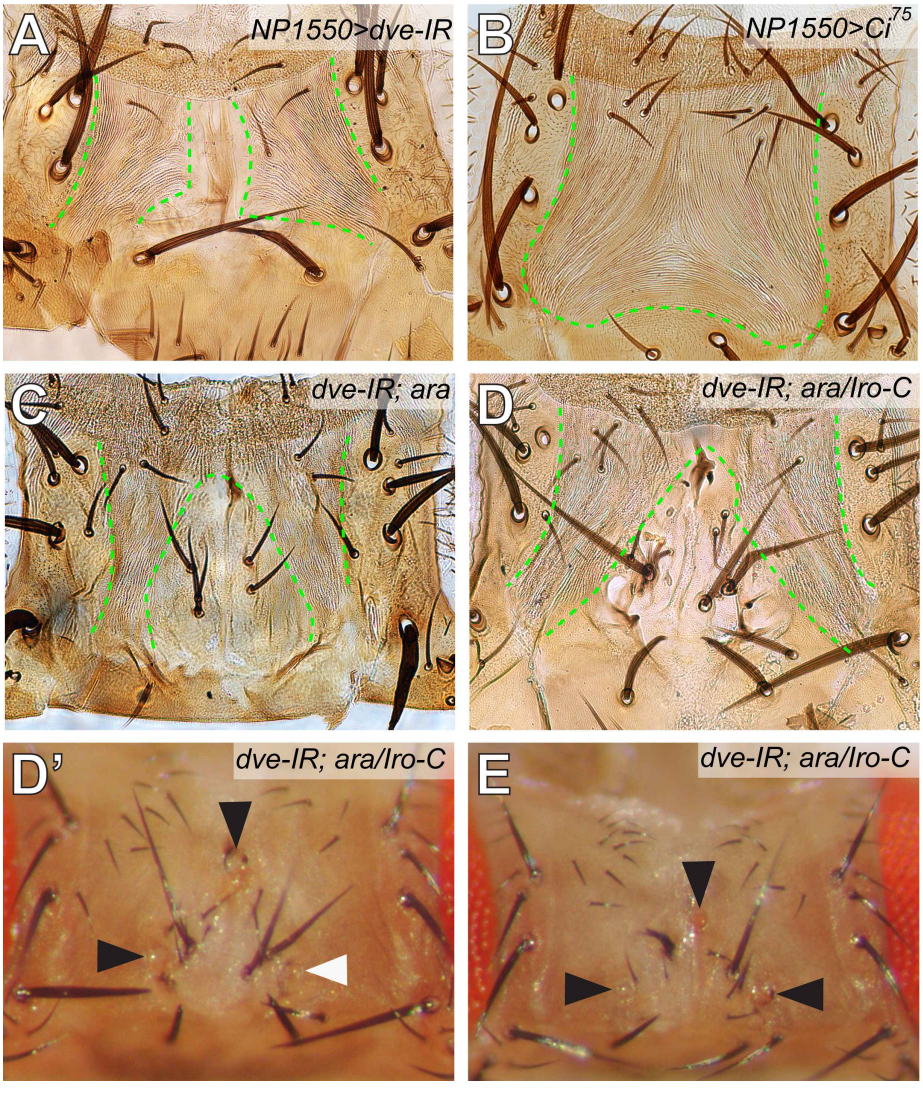
A
NP1550>dve-IR
B
NP1550>Ci75
C
dve-IR; ara
D
dve-IR; ara/Iro-C
D'
dve-IR; ara/Iro-C
E
dve-IR; ara/Iro-C

Fig. 6

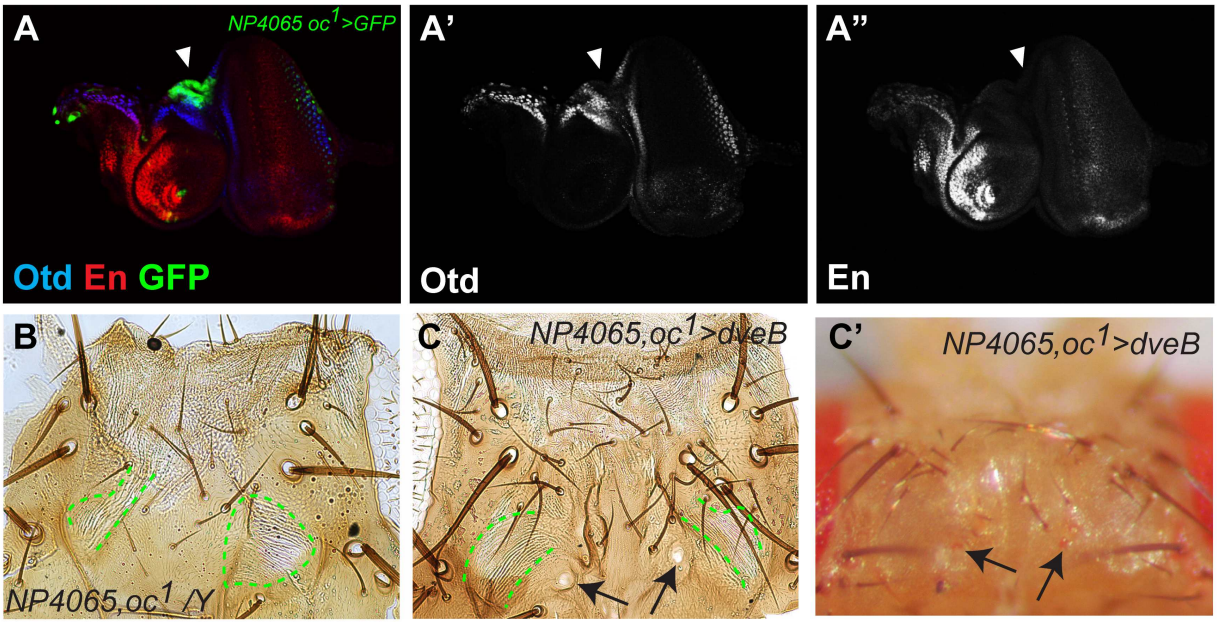
A
NP4065 oc1>GFP
Otd En GFP
A'
Otd
A''
En
B
NP4065,oc1 /Y
C
NP4065,oc1>dveB
C'
NP4065,oc1>dveB

Fig. 7

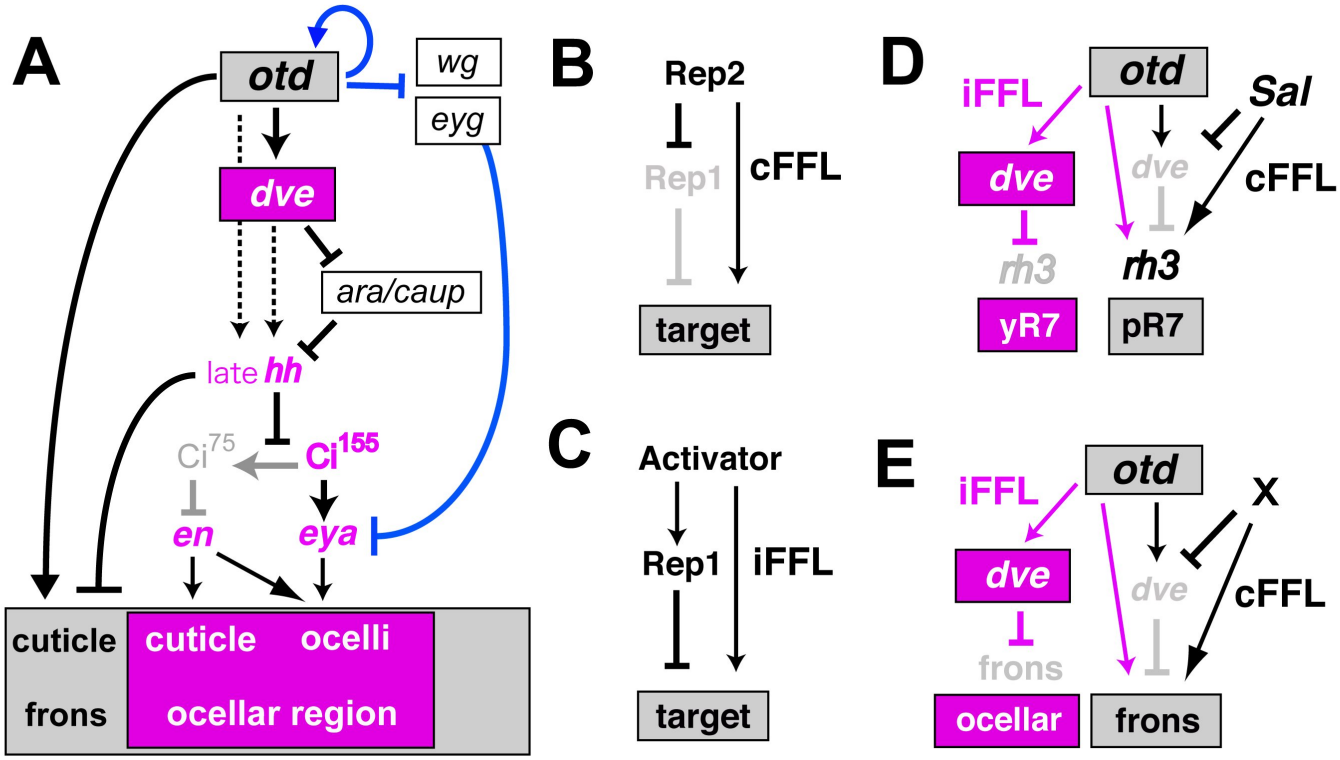
A
otd
wg
eyg
dve
ara/caup
late hh
Ci75
Ci155
en
eya
cuticle
frons
cuticle ocelli
ocellar region
B
Rep2
Rep1
cFFL
target
C
Activator
Rep1
iFFL
target
D
iFFL
otd
Sal
dve
dve
cFFL
rh3
rh3
yR7
pR7
E
iFFL
otd
X
dve
dve
cFFL
frons
ocellar
frons

Fig. 8

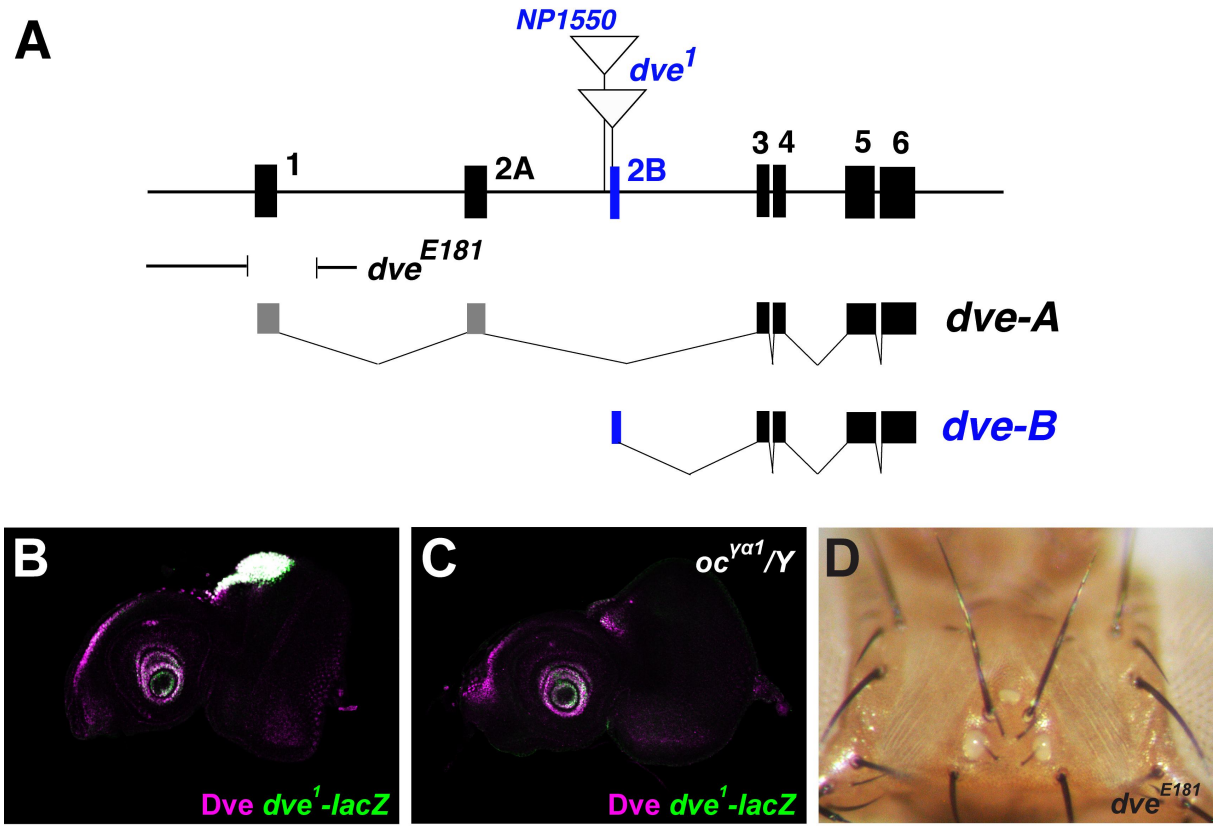
A
NP1550
dve1
1
2A
2B
3 4
5 6
dveE181
dve-A
dve-B
B
Dve dve1-lacZ
C
ocγα1/Y
Dve dve1-lacZ
D
dveE181

Fig. S1

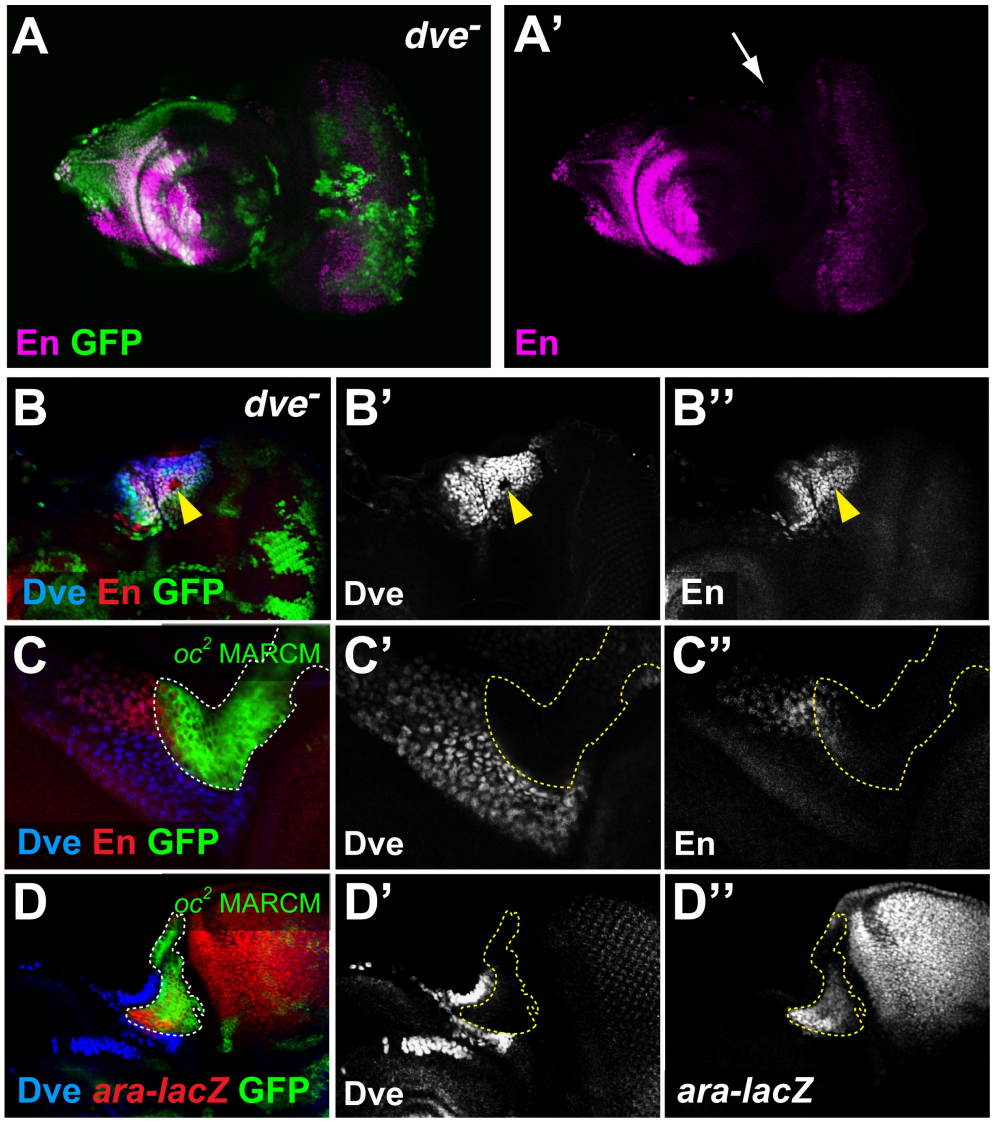
A
dve-
En GFP
A'
En
B
dve-
Dve En GFP
B'
Dve
B''
En
C
oc2 MARCM
Dve En GFP
C'
Dve
C''
En
D
oc2 MARCM
Dve ara-lacZ GFP
D'
Dve
D''
ara-lacZ

Fig. S2

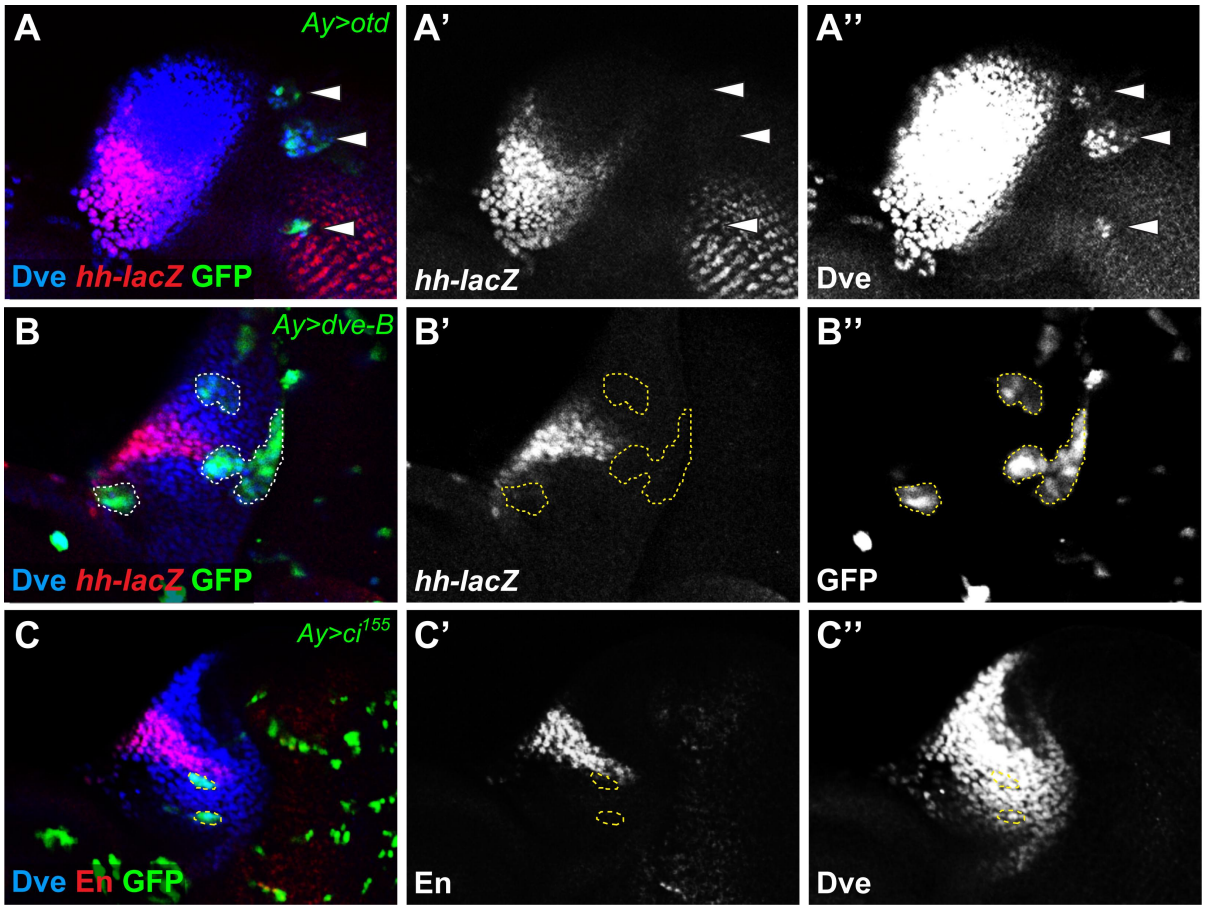
A
Ay>otd
Dve hh-lacZ GFP
A'
hh-lacZ
A''
Dve
B
Ay>dve-B
Dve hh-lacZ GFP
B'
hh-lacZ
B''
GFP
C
Ay>ci155
Dve En GFP
C'
En
C''
Dve

Fig. S3

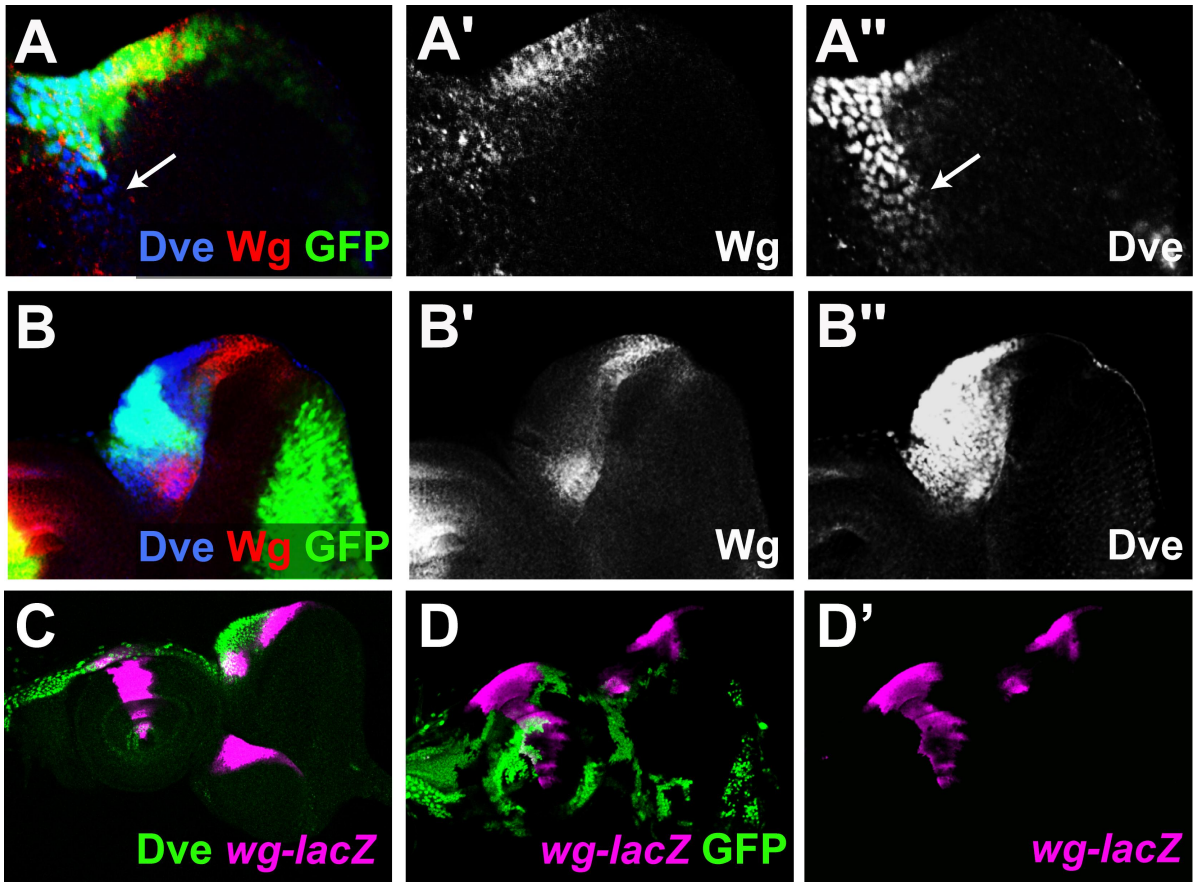
A
Dve Wg GFP
A'
Wg
A"
Dve
B
Dve Wg GFP
B'
Wg
B"
Dve
C
Dve wg-lacZ
D
wg-lacZ GFP
D'
wg-lacZ

Fig. S4